AIIM

Association for Information and Image Management

1100 Wayne Avenue, Suite 1100
Silver Spring, Maryland 20910

301/587-8202

Centimeter

1 2 3 4 5 6 7 8 9 10 11 12 13 14 15 mm

1 2 3 4 5

Inches

MANUFACTURED TO AIIM STANDARDS
BY APPLIED IMAGE, INC.

1 of 1

Conf-941046--1

LA-UR- 93-4305

Title: X-Ray Production with Sub-Picosecond Laser Pulses

Author(s): G.T. Schappert
J.A. Cobble
R.D. Fulton
G.A. Kyrala
G.L. Olson
A.J. Taylor

Submitted to: 11th International Workshop on Laser Interation and Related Plasma Phenomena

Monterey, CA
October, 1994

MASTER

Los Alamos
NATIONAL LABORATORY

Form No. 836 R5
ST 2629 10/91

X-RAY PRODUCTION WITH SUB-PICOSECOND LASER PULSES*

G. T. Schappert, J. A. Cobble, R. D. Fulton, G. A. Kyrala,
G. L. Olson and A . J. Taylor
Los Alamos National Laboratory
Los Alamos, NM 87545

ABSTRACT

The interaction of intense, sub-picosecond laser pulses with solid targets produces intense picosecond x-ray pulses. With focused laser pulses of several 10^{18} W/cm^2, He-like and H-like line radiation from targets such as aluminum and silicon has been produced. The energy conversion efficiency from the laser pulse energy to the 1-2 keV line x-rays is nearly one percent. The duration of the line x-ray radiation is of the order of ten picoseconds, although this may be an upper estimate because of the temporal resolution of the x-ray streak camera. The spatial extent of the x-ray source region is only slightly larger than the laser focal spot, or about 10 μm in diameter. With these characteristics, such x-ray sources emit an intensity of nearly 10^{14} W/cm^2. Experiments and modeling which led to the above conclusions will be discussed.

1. INTRODUCTION

The interaction of subpicosecond laser pulses with matter leads to the generation of intense short x-ray pulses. Results from experiments in the soft x-ray region, a few hundred eV [1-2] , as well as in the 1-2 keV region [3-6] have been published. In general, the primary motivation for this research has been to develop intense x-ray sources to pump x-ray lasers. Shortly after the invention of the laser it was proposed [7] that photo-pumped x-ray lasers should be possible provided a sufficiently intense x-ray pump source were available. Clearly, the shorter the wavelength of the x-ray laser, the higher is the intensity of the required x-ray pump flux. Another interesting application for such intense x-ray sources is the investigation of non-linear x-ray physics, for example two x-ray photon K shell ionization. In view of the extensive literature in this field, we will limit the discussion in this paper to the production of keV line radiation .

The physics involved in the x-ray generation is quite simple. A fraction of the incident laser energy is absorbed in the focal region, at the critical electron density, leading to a hot

* This work was performed under the auspices of the U. S. Department of Energy by the Los Alamos National Laboratory under contract No. W-7405-ENG-36.

electron plasma. The location of the critical density depends on whether the intense laser pulse is preceded by a prepulse. For no prepulse, the absorption takes place at the solid target interface and may be calculated using the Fresnel equations with a Drude model for the electrons. For a prepulse of sufficient intensity, an expanding plasma is established in front of the target and the major absorption of the main pulse, resonance absorption, occurs in this blow-off at the critical density. The prepulse plays an important role at this stage. It sets the scale length of the plasma density, the absorption, the amount of material in the absorption region and hence the peak electron temperature and density achieved. These conditions then determine the material charge state and hence the radiation. Within this scenario one should be able to generate a particular line spectrum by selecting an appropriate element, energy in the main laser pulse, and prepulse. Hence, the laser prepulse plays an important role in optimizing the conversion of the main pulse into x-rays[8-9].

With the energy deposited into the electrons, collisional ionization and excitation strip the material to charge states consistent with the plasma under highly transient non-LTE conditions. The line radiation results from radiative decay of excited states during the formation of the plasma and later during the subsequent recombination. Model calculations of this scenario will be presented and compared with the experimental results.

2. EXPERIMENTS

The experiments described in this section were carried out on the Los Alamos Bright Source II. This system is a XeCl excimer laser which amplifies a frequency doubled seed pulse generated by a synchronously pumped dye oscillator and amplifier . The detailed performance of this system is discussed in a previous paper[10]. In summary, the laser system operates at a wavelength of 308 nm, it produces a .3 ps pulse containing 0.25 Joules at a repetition rate of 1 Hz. When focused with f/1.8 optics, the irradiance on target can be as high as 5×10^{18} W/cm^2. The main pulse is preceded by a few ns long prepulse due to the ASE of the excimer amplifiers. Although its total energy is only 0.1-0.2 mJ , the resulting irradiance on target is on the order of 10^{11} W/cm^2 which is sufficient to generate a prepulse plasma in front of the target. To characterize the x-ray line production in the conversion region we determined the energy in the emitted spectral lines, imaged the area of the emission region, and measured the temporal history of the emission.

Figure 1 shows the He- and H-like Al line spectrum taken with a PET crystal spectrometer at a laser irradiance of a few 10^{18} W/cm^2. The spectrometer did not cover the He-like Al resonance line, but recorded a strong H-like resonance line and higher order He- and H-like lines. For comparison, figure 2 shows the same spectrum taken with our KrF system at about 10^{17} W/cm^2. The H-like lines are not as strong relative to the He-like lines as at the higher irradiance. Presumably, at a higher irradiance more energy is deposited in the interaction region leading to a higher electron temperature and hence faster excitation and ionization rates which lead to higher charge states. The total energy under the 1-2 keV line radiation in both spectra is about 1% of the incident laser energy . Similar results were obtained with Si targets.

Figure 3 shows the temporal history of the keV line radiation . It represents a line out

taken through an x-ray streak camera image filtered through 4 mills of Be. Although the camera has been calibrated in the UV with our sub-ps laser pulses to have a temporal response of about 4 ps[11], its temporal response to keV x-rays is usually somewhat slower, probably 8-10 ps. This gives an upper limit estimate of the keV x-ray pulse duration of about 10 ps.

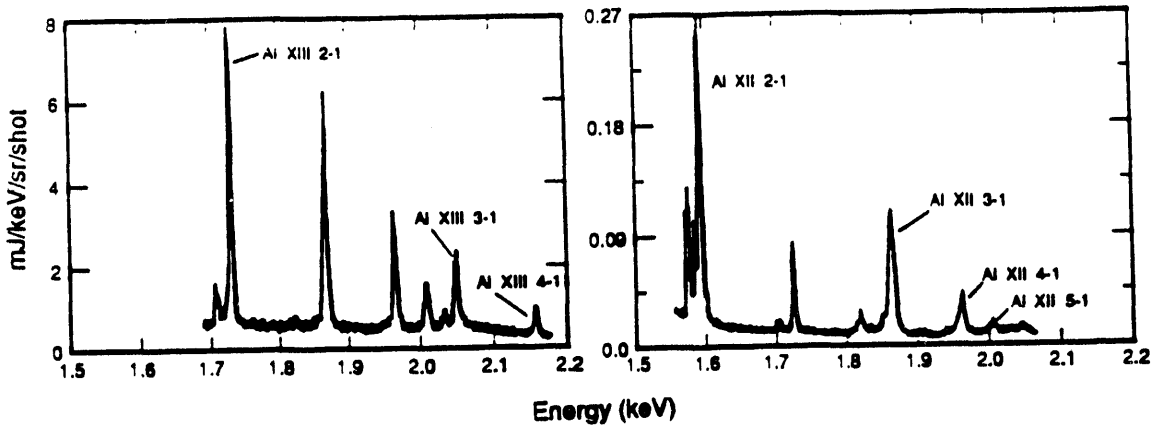

Figure 1. He- and H-like Al line spectra generated with XeCl laser pulses at a few 10^{18} W/cm^2 irradiance.

Figure 2 . He- and H-like Al line spectra generated with KrF laser pulses at 10^{17} W/cm^2 irradiance.

Figure 4 shows a contour plot of the image of the keV x-ray emission taken with a 7 μm diameter pinhole camera filtered through 1 mill of Be. The contours are in steps of 0.16 in the intensity, the first at 0.16 of peak. The radiation is taken to emanate from a disk which is viewed by the camera at an angle of 39° from the normal. The image has been corrected for this obliquity factor, resulting in fairly circular outer contours. After correcting for the pinhole dimension, the full width at half maximum of the keV radiation region is about 10μm . Combining the results of these measurements gives an estimate of the keV line x-ray emission from the conversion source of 10^{13}-10^{14} W/cm^2.

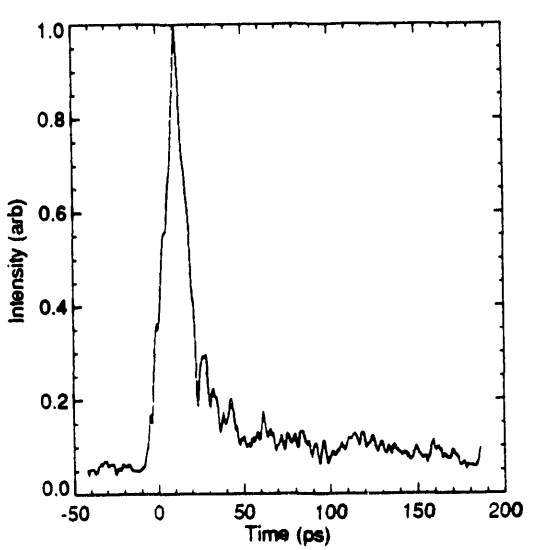

Figure 3. Streak camera image line-out of keV Al line radiation through 4 mill Be.

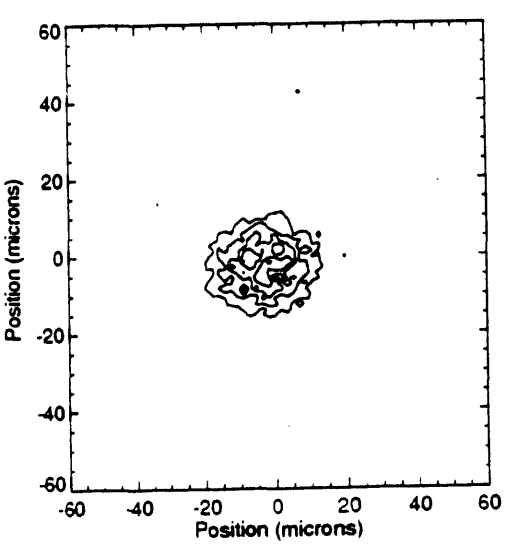

Figure 4. Contours of pinhole camera image through 1 mill Be.

3. MODELING

The above experimental results are modeled by a one-dimensional Lagrangian hydrodynamics code ZAP. This code calculates detailed atomic and radiation processes in a non-LTE highly transient plasma. The atomic data is generated with a family of Los Alamos codes based on Hartree-Fock wave functions to calculate energy levels, oscillator strengths, and electron impact excitation and ionization rates. Autoionization and di-electronic recombination is included by explicitly using doubly excited levels. To model plasmas produced by ultra-high intensity lasers, multi-photon ionization and multi-photon inverse bremsstrahlung is included. The atomic model used in a typical aluminum calculation contains 309 energy levels from the one ionized through the totally stripped atom. Configuration averaged levels are used for principle quantum numbers of 1, 2, and 3. In highly stripped ions, the n=4 levels are also configuration averaged. All other levels are Rydberg averaged. Doubly excited levels are added to the Be-, Li-, and He-like ions to calculate the appropriate satellite contributions to the spectra. Although the code is one-dimensional, the transverse thermal conduction which occurs in the real geometry is simulated through a lateral energy loss. The typical calculation then proceeds as follows.

For figures 5- 9 a prepulse starting at 1.3 x10^{11}W/cm^2 ramps up to 5.2x10^{11} W/cm^2 during 3 ns. Superimposed and centered at 3 ns is the main pulse, 114 mJ, .3 ps pulse width, at an intensity of 1.8x10^{18} W/cm^2. The absorption of the prepulse is inverse-bremsstrahlung starting with the solid Al surface as singly ionized Al at room temperature. This starts the prepulse expansion. The main pulse propagates through the prepulse plasma, is attenuated through inverse-bremsstrahlung and multiphoton absorption. At the critical electron density surface 50% is absorbed through resonance absorption, the rest reflected.

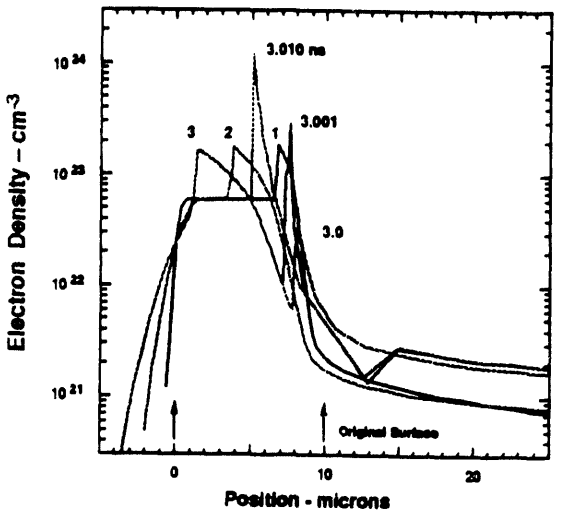

Figure 5. Calculated electron density as a function of position at various times

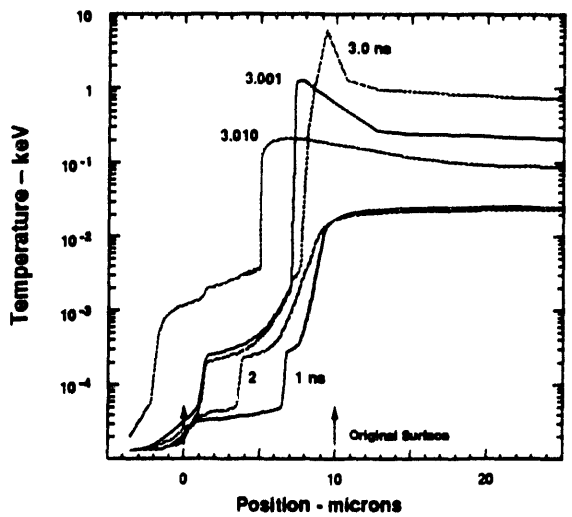

Figure 6. Calculated electron temperature as a function of position at various times

Figures 5 and 6 show the electron density and temperature respectively as a function of position for various times. The target is a 10 μm Al foil, the original front surface is

located at 10 μm and the back at 0 μm. The curves marked 1 and 2 ns show the prepulse plasma blow-off and shock waves propagating into the foil. At 3 ns the shocks into the foil continue, but a spike in the electron density develops at the critical density where the pulse is absorbed. This spike is due to the rapid further ionization and the radiation pressure of the pulse. At the same time an outward moving rarefaction develops as seen at about 13 μm. At 3.001 ns the main pulse energy deposition is completed but the hot plasma ionizes further, reaching a peak electron density of about 10^{24} electrons/cm^3. This is equivalent to slightly compressed totally stripped solid Al.

The electron temperature in Figure 6 follows a similar pattern. The curves at 1 and 2 ns show the temperature profile in the blow-off plasma and the solid target. At 3 ns half of the main pulse energy is deposited, reaching an electron temperature of 6 keV in the deposition zone. The energy quickly diffuses, and by 10 ps after the main pulse the region has cooled to 100 eV. The calculated peak temperature of 6 keV is probably too high and finer zoning in the absorption region would bring it down somewhat. However, electron temperatures in the 1-2 keV range are required to obtain sufficiently fast ionization and excitation rates to produce the observed He- and H-like line radiation.

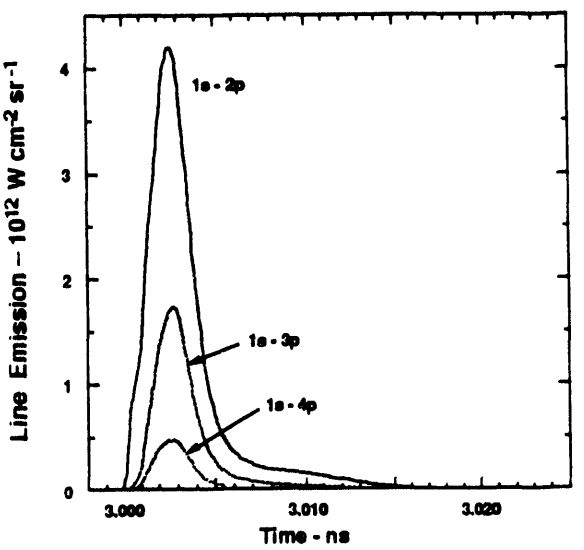

Figure 7. Calculated time dependence of H-like Al line emission

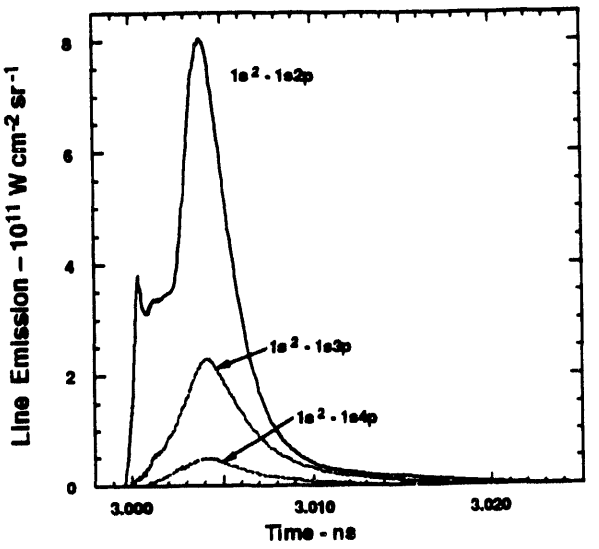

Figure 8. Calculated time dependence of He-like Al line emission

Figures 7 and 8 show the calculated time dependence of the H- and He-like Al line radiation respectively. Note at first the He-like resonance line intensity increases rapidly, but then takes a dip when the H-like resonance line comes in. That is, the plasma has burned through the He-like charge state. Note further that the H-like line intensities reach a maximum about 3 ps after the main laser pulse. This reflects the fact that it takes time to excite and ionize the material. As the H-like intensities decrease, the He-like lines come back as recombination through the He-like levels occurs. The full width at half maximum of these lines is within 3-6 ps. This is shorter than our streak images, although not necessarily inconsistent because of the temporal resolution of the camera. The peak intensity radiated

from the target is 2π times what is shown on the figures, or mid 10^{13} W/cm^2. This the same as the estimate from the experimental results. The total energy radiated in the H- and He-like lines is about 2% of the incident laser energy, all based on per cm^2 since the calculation is one-dimensional. Again this compares quite well with the 1% estimate from the experimental results.

Figures 9 and 10 show the calculated time integrated line spectra of the He- and H-like Al emission. The spectrum in figure 9 is based on the above calculations for the short pulses from our XeCl system at 1.8×10^{18} W/cm^2. Figure 10 results from the same calculation but at an irradiance of 7×10^{16} W/cm^2 to simulate the experimental comparison between figures 1 and 2. The spectral lines are transported through the plasma, adaptively binned to resolve the line structure, and then convolved with a 0.8 eV Lorentzian to simulate an instrument function for the spectrometer. Qualitatively, the calculation agrees with the experimental observation that the higher irradiance shifts the ionization to more H- than He-like as expected. A quantitative comparison for the peak He- to H-like line intensity ratios between the two irradiances agrees to within a factor of 2.

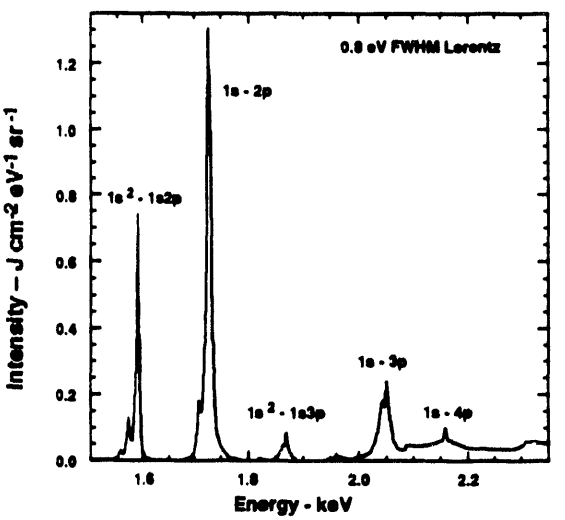

Figure 9. Calculated time integrated H- and He-like Al spectra at 1.8×10^{18} W/cm^2 irradiance

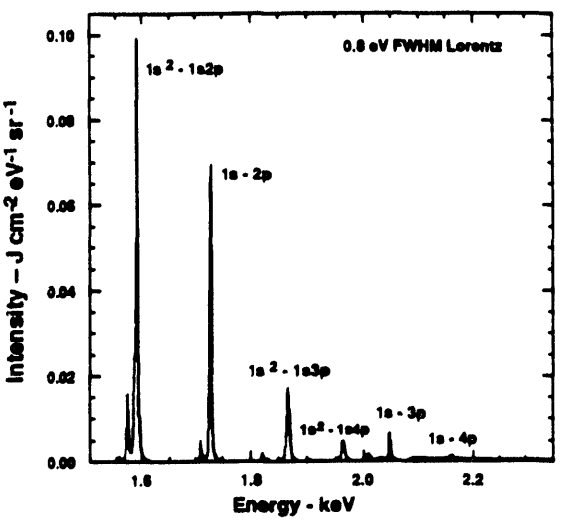

Figure 10. Calculated time integrated H- and He-like Al spectra at 7×10^{16} W/cm^2 irradiance

4. CONCLUSION

We have experimentally characterized the generation of line x-rays in the interaction of subpicosecond laser pulses with solid targets. The experiments concentrated on the He- and H-like lines of aluminum. We have measured the spectrum and the energy in the lines. The time history of the emission of individual lines could not be measured since there is not enough intensity to streak and image the spectrum. However, the time history of the emission above 1 keV, which consists primarily of the lines of interest, could be measured with a temporal resolution of about 10 ps. The emission region was imaged with a pinhole camera. From

these measurements we conclude that the interaction of the subpicosesond laser pulses with an irradiance of 10^{18} W/cm^2 on a prepulsed solid target can generated a line x-ray source with an emittance approaching 10^{14} W/cm^2.

The experimental results were compared with model calculations using a one-dimensional hydrocode containing detailed appropriate atomic physics, atomic rates, and transport processes. Where a comparison was possible, the agreement was generally with in a factor of two. Given the complexity of the calculation and the precision to which the experimental results can be determined , this agreement is acceptable. We conclude that we have a reasonably consistent picture of the generation of line x-ray emission from solid targets.

5. REFERENCES

1. M. M. Murnane, H. C. Capteyn, and R. W. Falcone Phys. Rev. Lett. **62**, 155, 1989
2. Margaret M. Murnane, Henry C. Kapteyn, Mordecai D. Rosen, Roger W. Falcone **Science 251,** 531, 1991
3. J. A. Cobble, G. A. Kyrala, A. A. Hauer, A. J. Taylor, C. C. Gomez, N. D. Delamater, and G.T. Schappert, Phys. Rev. A, **39,** 453, 1989
4. G. A. Kyrala, R. D. Fulton, E. K. Wahlin, L. A. Jones, G. T. Schappert, J. A. Cobble, and A. J. Taylor, Appl. Phys. Lett. **60,** 2195, 1992
5. W. H. Goldstein, A. Ziegler, P. G. Burghalter, D. J. Nagel, A. Bar-Shalom, J. Oreg, T. S. Luk, A. McPherson, and C. K. Rhodes, Phys. Rev. E **47,** 4349, 1993
6. J. C. Kieffer, M. Chaker, J. P. Matte, H. Pepin, C. Y. Cote, Y. Beaudoin, C. Y. Chien, S. Coe, G. Mourou, and O. Peyrusse, Phys. Fluids **B5,** 1,1992
7. M. A. Duguay and P. M. Rentzepis, Appl. Phys. Lett. **10,** 350, 1967
8. J. A. Cobble, G. T. Schappert, L. A. Jones, A. J. Taylor, G. A. Kyrala, and R. D. Fulton J.Appl. Phys, **69**, 3369, 1991
9. U. Teubner, G. Kühnle, and F. P. Schäfer, Appl. Phys. Lett. **59,** 2672,1991
10. A. J. Taylor, C. R. Tallman, J. P. Roberts, C. S. Lester, T. R. Gosnell, P. H. Y. Lee and G. A. Kyrala, Opt. Lett. **15**, 39 (1990)
11. J. A. Cobble, R. D. Fulton, L. A. Jones, G. A. Kyrala, G. T. Schappert, A. J. Taylor and E. K. Wahlin
    Rev. Sci. Instrum, **63** (10), 5116, (1992)

DATE
FILMED
9/15/94

END